

Pure and Saturated Red Electroluminescent Polyfluorenes with Dopant/Host System and PLED Efficiency/Color Purity Trade-Offs

By Lei Chen, Baohua Zhang, Yanxiang Cheng, Zhiyuan Xie, Lixiang Wang,* Xiabin Jing, and Fosong Wang

Three kinds of red electroluminescent (EL) polymers based on polyfluorene as blue host and 2,1,3-benzothiadiazole derivatives with different emission wavelengths as red dopant units on the side chain are designed and synthesized. The influence of the photoluminescence (PL) efficiencies and emission wavelengths of red dopants on the EL efficiencies and color purities of the resulting polyfluorene copolymers of dopant/host system is investigated by adjusting the electron donating ability of the donor units in D- π -A-D typed 2,1,3-benzothiadiazole derivatives. The devices of these red-emitting polymers realize remarkable EL efficiency/color purity trade-offs. The single-layer devices with the configuration of ITO/PEDOT:PSS/Polymer/Ca/Al show pure red emission at 624 nm with a luminous efficiency of 3.83 cd A⁻¹ and CIE of (0.63, 0.35) for PFR1, saturated red emission at 636 nm with a luminous efficiency of 2.29 cd A⁻¹ and CIE of (0.64, 0.33) for PFR2, respectively. By introduction of an additional electron injection layer PF-EP(Ethanol soluble phosphonate-functionalized polyfluorene), high performance pure and saturated red emission two-layer devices (ITO/PEDOT:PSS/Polymer/PF-EP/LiF/Al) were achieved with maximum luminous efficiencies of 5.50 cd A⁻¹ and CIE of (0.62, 0.35) for PFR1, 3.10 cd A⁻¹ and CIE of (0.63, 0.33) for PFR2, respectively, which are the best results for pure and saturated fluorescent red EL polymers reported so far.

1. Introduction

Since the pioneering work of Burroughes et al. in 1990,^[1] polymer light emitting diodes (PLEDs) based on conjugated polymers have attracted widely research interest for their potential applications in full color flat-panel displays and illuminations.^[2–6]

[*] Dr. L. Chen, Dr. B. Zhang, Prof. Y. Cheng, Prof. Z. Xie, Prof. L. Wang, Prof. X. Jing, Prof. F. Wang
State Key Laboratory of Polymer Physics and Chemistry
Changchun Institute of Applied Chemistry
Chinese Academy of Sciences
Changchun 130022 (P. R. China)
E-mail: lixiang@ciac.jl.cn
Dr. L. Chen, Dr. B. Zhang
Graduate School of the Chinese Academy of Sciences
Beijing 100039 (P. R. China)

DOI: 10.1002/adfm.201000840

Compared to inorganic and small molecular organic light-emitting diodes, PLEDs can be conveniently manufactured by solution processing techniques such as spin coating or ink-jet printing, which is very important for low cost, flexible and large-area displays. For full color displays, three basic color-red, green and blue are required. Compared with green and blue emissive polymers, the development of red EL conjugated polymers is far behind in terms of both color purity and EL efficiency. Most red-emitting conjugated polymers are realized by incorporating red fluorophores, such as 2,1,3-benzothiadiazole derivatives,^[7–9] 2,1,3-benzoselenadiazole derivatives,^[9–11] 2,1,3-naphthaselenadiazole,^[12] cyanovinyl-containing units,^[13,14] 3,4-diphenylmaleimide derivatives^[15] and phenothiazine derivatives,^[16] perylene-containing dyes,^[17] etc., into backbones, side chains or end groups of conjugated polymers. Due to the nature of red emissive materials, the red fluorophores emitting longer wavelength are more extensively π -conjugated or stronger polar compounds, which usually have lower fluorescence quantum yields (Φ_{PL}). Meanwhile, they are highly susceptible to concentration quenching in solid state because of the intermolecular dipole–dipole interactions or π – π stacking.^[18] So, the devices of red polymers with red enough emission wavelengths to achieve excellent CIE coordinates usually show inferior EL efficiencies. Until now, all of the fluorescent pure and saturated red-emitting polymers show EL efficiencies no more than 2.0 cd A⁻¹.^[12,16,19,20]

Recently, our group has reported a new approach to design high efficiency EL polymers of dopant/host system with molecular dispersion feature by covalently attaching small amounts of dopant units to the side chain of polyfluorene host.^[21–25] By this means, the problems of phase separation in physical blend material systems^[26–28] and voltage dependence of the EL spectrum existing in multilayer devices^[29–32] will be avoided due to the homogeneous distribution of the dopant units in the polymer host. Meanwhile, the concentration quenching effect aforementioned will be partly suppressed because of the low

quantum yields (Φ_{PL}). Meanwhile, they are highly susceptible to concentration quenching in solid state because of the intermolecular dipole–dipole interactions or π – π stacking.^[18] So, the devices of red polymers with red enough emission wavelengths to achieve excellent CIE coordinates usually show inferior EL efficiencies. Until now, all of the fluorescent pure and saturated red-emitting polymers show EL efficiencies no more than 2.0 cd A⁻¹.^[12,16,19,20]

content of dopant units, so highly efficient blue,^[21] green,^[22] red^[23] and white^[24,25] PLEDs have been realized by using dopant/host strategy. However, for red-emitting polymers,^[23] the key problem in our previous report is that we haven't realized the EL efficiency/color purity trade-offs. We find that highly efficient PLED (5.10 cd A⁻¹) is not red enough (orange-red emission at 615 nm, CIE of (0.59, 0.39)), and deep-red PLED at 645 nm is not so efficient (1.70 cd A⁻¹), which is clearly corresponding to the PL efficiencies and emission wavelengths of the red dopant units. Thus, optimization of red dopant units is very important for realizing red PLEDs EL efficiency/color purity trade-offs.

In this article, we report a series of red EL polymers based on polyfluorene as blue host and 2,1,3-benzothiadiazole derivatives with fine-tuned PL efficiencies and emission wavelengths as red dopant units on the side chain, aiming at tuning the EL efficiencies and color purities of the resulting polyfluorene copolymers of dopant/host system and realizing the optimization of red PLEDs EL efficiency/color purity trade-offs. The difference between this article and previous study is on achieving excellent PLEDs EL efficiency/color purity trade-offs for red fluorescent polymers based on polyfluorene as blue host and 2,1,3-benzothiadiazole derivatives as red dopant. As a result, the single-layer devices of these polymers (ITO/PEDOT:PSS/Polymer/Ca/Al) show pure red emission at 624 nm with a luminous efficiency of 3.83 cd A⁻¹ and CIE of (0.63, 0.35) for PFR1, and saturated red emission at 636 nm with a luminous efficiency of 2.29 cd A⁻¹ and CIE of (0.64, 0.33) for PFR2 respectively. Furthermore, by using ethanol soluble phosphonate-functionalized polyfluorene (PF-EP) as the electron injection layer (EIL) reported in our previous study,^[33] high performance two-layer devices (ITO/PEDOT:PSS/Polymer/PF-EP/LiF/Al) are obtained with maximum luminous efficiencies of 5.50 cd A⁻¹ and CIE of (0.62, 0.35) for pure red emission (PFR1), and 3.10 cd A⁻¹ and CIE of (0.63, 0.33) for saturated red emission (PFR2), respectively. To the best of our knowledge, these are the highest efficiencies of pure and saturated red fluorescent EL polymers reported so far.

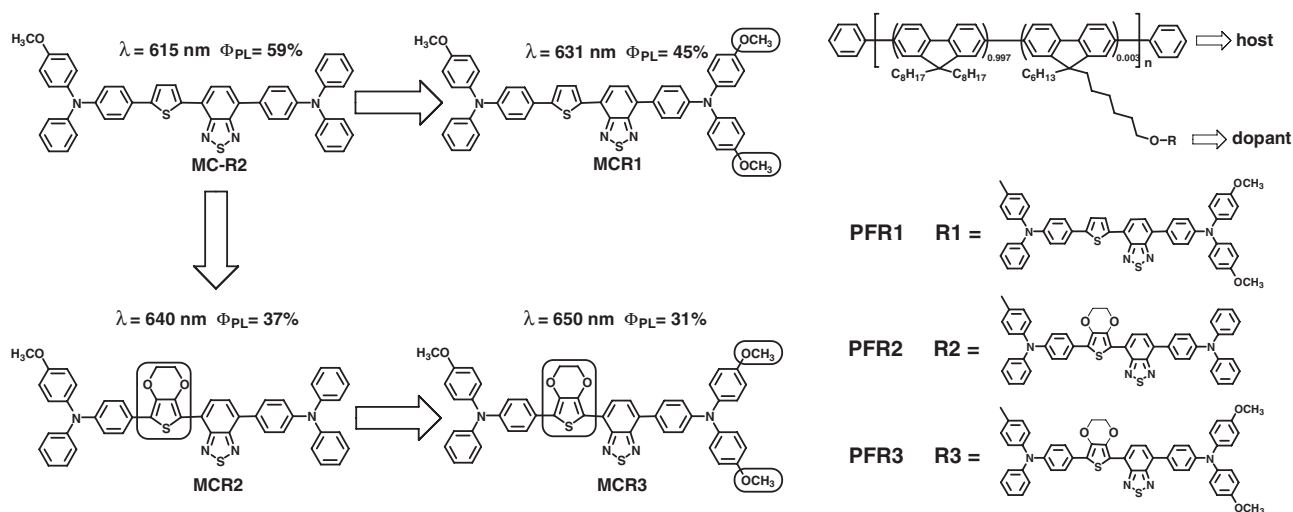
2. Result and Discussion

2.1. Molecular Design

We designed a series of saturated red emission model compounds (MCs), as shown in **Scheme 1**, by introducing different alkoxy groups to increasing the electron donating ability of 4-(5-(4-(*N*-phenyl-*N*-(4-methoxy)phenylamino)phenyl)thienyl)-2-(7-(4-(diphenylamino)phenyl)-2,1,3-benzothiadiazole) (MC-R2) reported in our previous work, which show high PL efficiency (59%), but orange-red emission at 615 nm. Firstly, we designed MCR1 by incorporating two methoxy groups to the triphenylamine segment of MC-R2, which will lead to about 10 nm redshift according to our experience.^[24,34] Secondly, we designed MCR2 by changing the thiophene unit of MC-R2 to 3,4-ethylenedioxythiophene (EDOT) unit, which will lead to more than 10 nm redshift due to the stronger electron-donating effect of the ethylenedioxy bridge compared to dialkoxy groups.^[35] Thirdly, for comparison, we designed MCR3 by adopting above-mentioned two modifications at the same time. Thus, we hope to obtain saturated red dopants with fine-tuned PL efficiencies and emission wavelengths. Then we obtained red polymers through covalently attaching these red dopant units to the side chain of polyfluorene using alkyl spacers. The contents of the red dopant units have been controlled to be 0.3 mol% in order to achieve almost complete energy transfer from polyfluorene host to red dopant units and suppress the concentration quenching effect. Thus, high EL efficiencies of these polymers with superior CIE coordinates will be expected.

2.2. Synthesis and Characters

The synthetic routes of the red MCs, monomers and corresponding polymers are outlined in **Scheme 2**. The tert-butyltrimethylsilyl (TBS) group protected intermediates were all synthesized by Stille coupling. The TBS groups are stable



Scheme 1. Chemical structure of red model compounds and polymers.

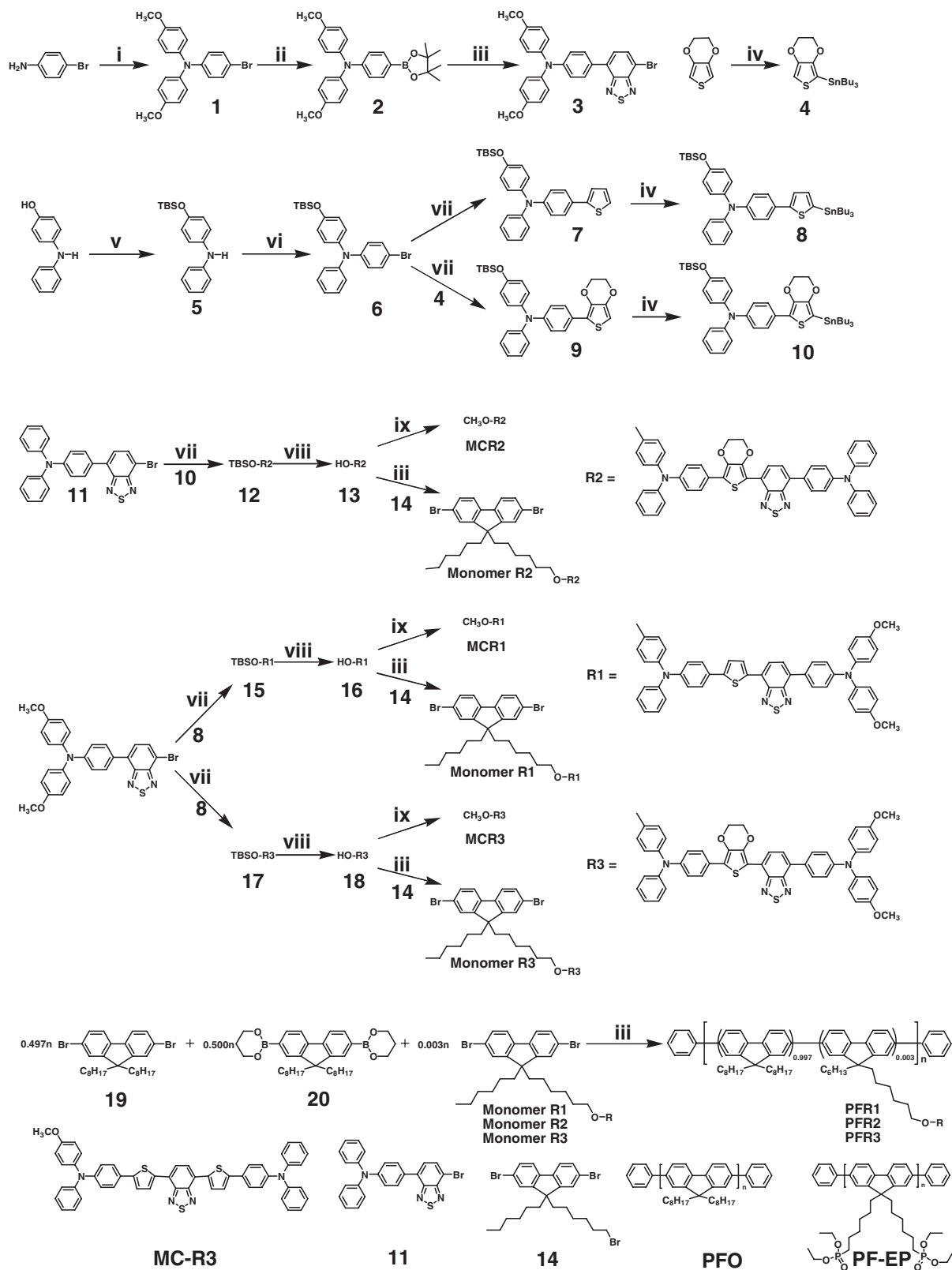


Table 1. Photophysical, electrochemical properties, and energy levels of the RMCs.

	λ_{abs} [nm] [a]	λ_{emi} [nm]	Φ_{PL} [%]	$E_{\text{ox}}^{\text{onset}}$ [V] [b]	E_{HOMO} [eV]	$E_{\text{red}}^{\text{onset}}$ [V]	E_{LUMO} [eV]	E_{g} [eV]
MCR1	511	631	49	0.71	-5.05	-1.20	-3.14	1.91
MCR2	519	640	37	0.67	-5.01	-1.21	-3.13	1.88
MCR3	529	650	31	0.63	-4.96	-1.23	-3.11	1.85

[a] Measured in around 10^{-6} M toluene solution. [b] Measured in 10^{-3} M CH_2Cl_2 solution, $n\text{-Bu}_4\text{NClO}_4$ as supporting electrolyte.

to $n\text{-BuLi}$ and could be easily deprotected using aqueous HCl without affecting other alkoxy groups to get corresponding hydroxylated intermediates, which were then methylated by CH_3I to synthesize the three red MCs: MCR1, MCR2, and MCR3. The hydroxylated intermediates could also react with 2,7-dibromo-9-hexyl-9-(6-bromohexyl)fluorene (14) to afford the three red monomers, Monomer R1, Monomer R2 and Monomer R3 with high yields. All the red polymers were synthesized by classic palladium-catalyzed Suzuki polycondensation of 2,7-dibromo-9,9-dioctylfluorene (19), 2,7-bis(trimethyleneborate)-9,9-dioctylfluorene (20) and the corresponding red monomers and sequentially end-capped by phenylboronic acid and bromobenzene. The number-average molecular weights (M_n) of PFR1, PFR2 and PFR3, as determined by gel permeation chromatography (GPC) with polystyrene as standards, range from 36 700 to 53 400 with polydispersities (PDI) ranging from 2.52 to 2.91. All these polymers show good thermal stability as PFO with thermal degradation temperature (T_d) around 430 °C (Table 1).

2.3. Electrochemical Properties

Cyclic voltammetry measurements have been demonstrated to investigate the energy levels of the three red MCs, the results are shown in Figure 1a. Their onset oxidation voltages and onset reduction voltages as well as the highest occupied molecular orbital (HOMO) and lowest unoccupied molecular orbital (LUMO) energy levels are listed in Table 1, which clearly shows that both of the HOMO and LUMO energy levels of the three model compounds are increased due to enhanced electron donating abilities of donor units, but the increasing amplitudes of the HOMO energy levels are higher than the LUMO energy levels. As shown in Figure 1b, the HOMO and LUMO energy levels of all the three model compounds are located between those of PFO, as a result, effective charge trapping of the red dopants in the EL process will be expectable.

We also explored the electrochemical properties of all the polymers films spin-coated on a glassy-carbon working electrode. As shown in Table 2, incorporating a small amount of red dopant units to the side chain of PFO almost doesn't affect the electrochemical properties of the resulting polymers, which have similar HOMO and LUMO energy levels as PFO.

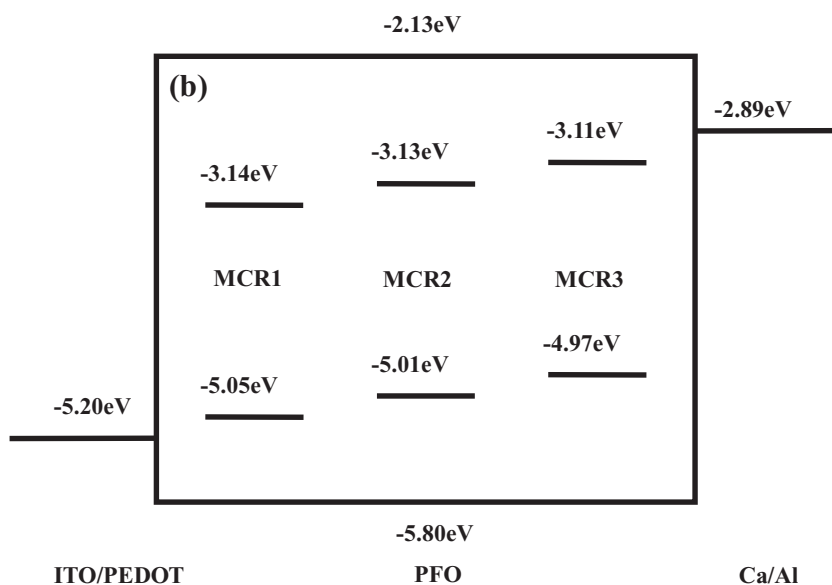
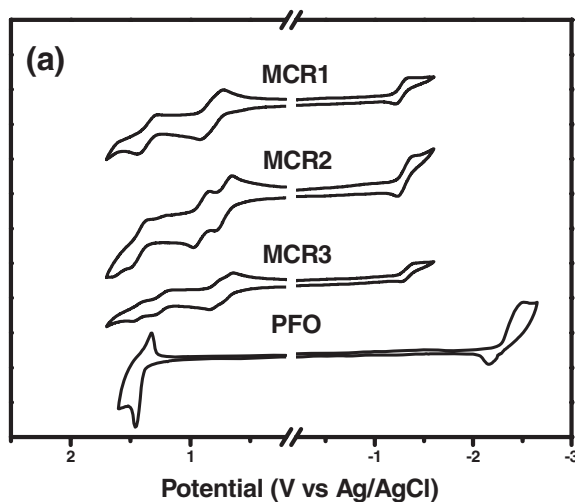


Figure 1. Cyclic voltammetry (a) and energy levels (b) of model compounds and PFO.

Table 2. Characters of the red polymers and PFO.

	M_n ($\times 10^4$)	PDI	T_d [$^{\circ}\text{C}$]	$E_{\text{onset}}^{\text{oxid}}$ [V] [a]	E_{HOMO} [eV]	$E_{\text{red}}^{\text{onset}}$ [V]	E_{LUMO} [eV]
PFO	4.1	2.5	430	1.37	-5.80	-2.30	-2.13
PFR1	4.7	2.6	433	1.37	-5.80	-2.32	-2.11
PFR2	3.7	2.9	431	1.38	-5.81	-2.32	-2.11
PFR3	5.3	2.5	430	1.38	-5.81	-2.33	-2.09

[a] Measured in film state, using 0.1 M n-Bu₄NClO₄ in CH₃CN as supporting electrolyte solution.

2.4. Photophysical Properties

Figure 2 shows the absorption spectrum and PL spectrum of the three red MCs, their corresponding peak emission wavelengths are listed in Table 2. Comparing with MC-R2, the introduction of two methoxy groups (MCR1) leads to 12 nm red-shift of absorption spectrum and 11 nm red-shift of PL spectrum, alternating thiophene unit by EDOT unit (MCR2) leads to 20 nm red-shift of absorption spectrum and 20 nm red-shift of PL spectrum, respectively. MCR3 has another 10 nm redshift of both absorption spectrum and PL spectrum compared to

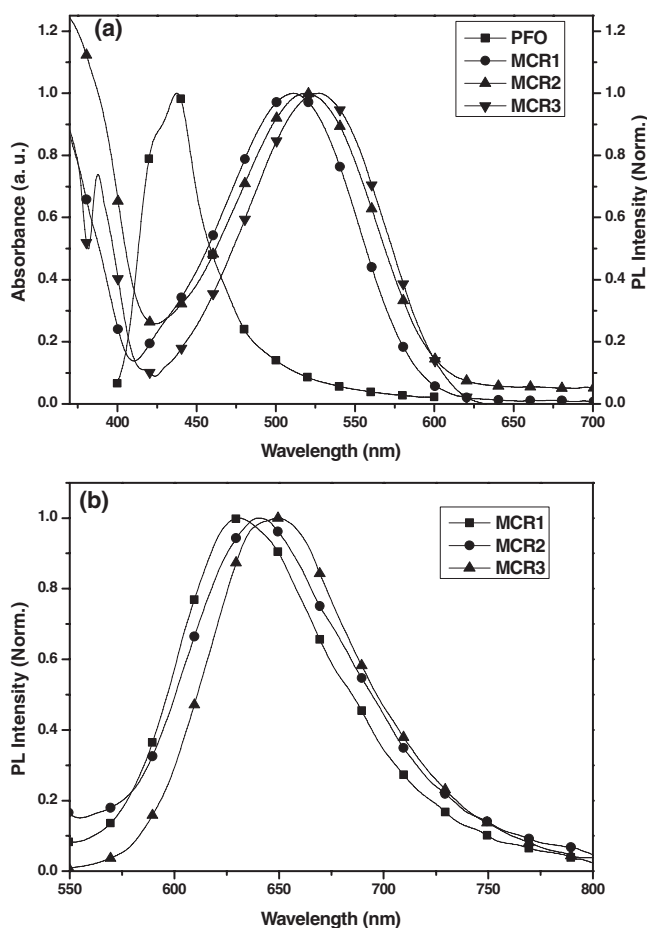


Figure 2. Absorption spectra of RMCs in dilute toluene solution and PL spectrum of PFO in film state (a) and PL spectra of RMCs in dilute toluene solution (b).

MCR2. More importantly, all of them show saturated red emission with high Φ_{PL} values in dilute toluene solution (listed in Table 2). The results coincide with our expectation very well, demonstrating that our molecular design can really obtain saturated red dopants with fine-tuned PL efficiency/emission wavelength trade-offs. We find that MCR2 and MCR3 have similar emission wavelengths but higher Φ_{PL} values (37% and 31%) compared to the deep-red MC-R3 (24%, see in Scheme 2) reported in our previous work, indicating that it is a better choice to realize longer wavelength emission by alternating π -conjugated thiophene unit by alkoxy groups. It's probably due to the heavy atom effect of the sulfur atom^[36,37] and/or the decrease of rigidity of the molecule with more thiophene units, both of which will lead to more nonradiative decay process and lower PL quantum yield for MC-R3. As shown in Figure 2a, the absorption spectrum of all these red MCs have good overlap with the PL spectrum of PFO, so efficient Förster energy transfer from polyfluorene host to red dopant units in PL and EL processes is expected.

The absorption spectra of PFR1, PFR2, PFR3 and PFO in films are shown in Figure 3a. All the red polymers exhibit similar absorption spectra as PFO with a peak absorption wavelength at 393 nm attributed to the π - π^* transition of the polyfluorene backbone, and there are no obvious signals of the charge transfer state absorption of the red dopant units at around 511 nm/519 nm/529 nm. Figure 3b shows the PL spectra of the polymers in films with an excitation wavelength at 380 nm. The PL spectra of all the red polymers exhibit not only blue emission from the polyfluorene backbone but also red emission from the dopant units. Since the absorption of the red dopant units in the polymers almost can't be detected, we attribute the red emission of the polymers to the efficient Förster energy transfer from polyfluorene host to the red dopant units in the PL process. Furthermore, the relative intensity of red emission for PFR1, PFR2, and PFR3 decrease successively, mainly due to the PL quantum efficiencies of the three red dopant units and the spectral overlap between the PL spectrum of polyfluorene host and the absorption spectra of the three red dopant units decrease sequentially as well.

2.5. EL Properties

In order to investigate the EL properties of the red polymers, we fabricated single-layer devices with a configuration of ITO/PEDOT:PSS(40 nm)/Polymer(90 nm)/Ca(10 nm)/Al(100 nm). Unlike the PL spectra, the EL spectra of all the polymers predominantly exhibit pure red emission attributed to the red dopant

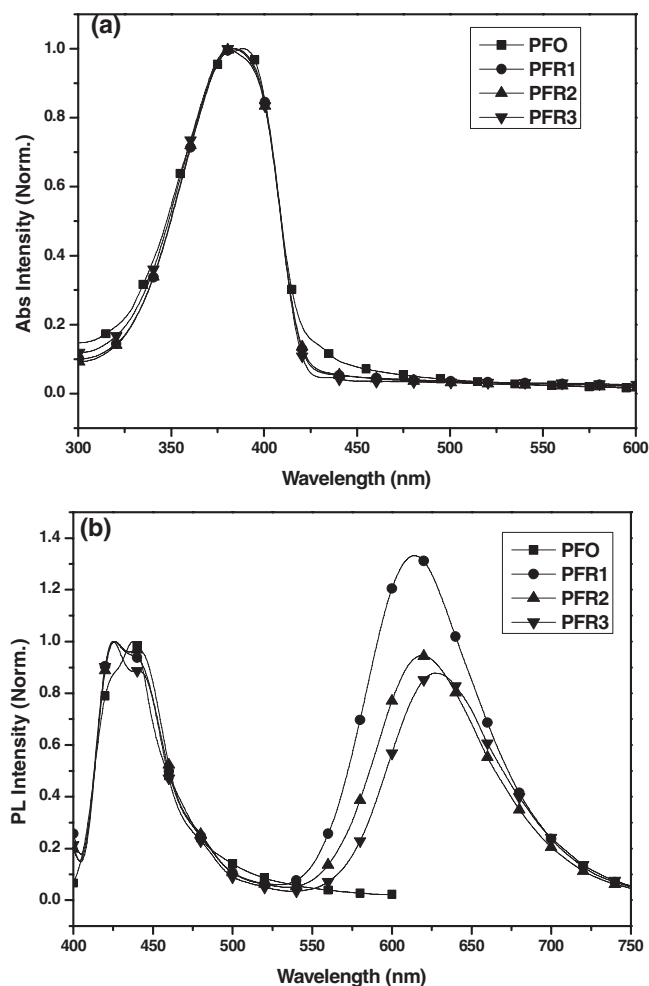


Figure 3. Absorption (a) and PL (b) spectrum of the red polymers and PFO in film states.

units with negligible blue emission from polyfluorene backbone (Figure 4a). It's because there is only Förster energy transfer from polyfluorene to the red dopants in the PL process. While, in the EL process, the direct charge trapping on the red dopant units also contribute to the red emission due to their LUMO/HOMO energy levels lie between the LUMO/HOMO energy levels of polyfluorene. All the polymers show pure red emission with maximum emission wavelengths at 624 nm, 636 nm, and 652 nm for PFR1, PFR2, and PFR3, respectively (Table 3). The CIE coordinates of the devices of these polymers are

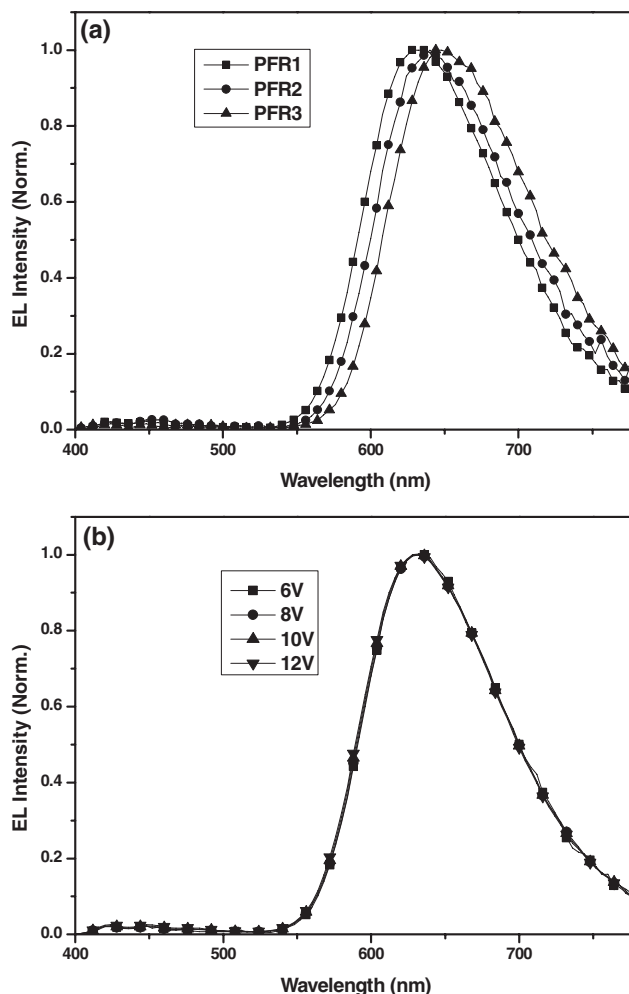


Figure 4. EL spectra of the devices of the red polymers (a) and EL spectra at different voltages of the device of PFR1 (b).

demonstrated to be (0.63, 0.35), (0.64, 0.33), (0.65, 0.32), which are close to the standard red (0.64, 0.33) demanded by the European Broadcasting Union (EBU). Moreover, the EL spectral shape of the devices of these polymers keeps almost unchanged at different voltages, just like the EL spectra of PFR1 shown in Figure 4b. Meanwhile, the CIE chromaticity coordinates of the device of PFR1 just change from (0.635, 0.352) at 6.5 V to (0.625, 0.351) at 12.0 V.

Table 3 outlined the EL performance of the single-layer devices of the red polymers. All the devices of these

Table 3. EL performance of the single layer devices of the red polymers.

	Turn-on Voltage [V] [a]	Luminous Efficiency [cd A^{-1}] [b]	Power Efficiency [lm W^{-1}] [c]	Maximum Brightness [cd m^{-2}]	λ_{max} [nm]	CIE (x, y) [d]
PFR1	6.5	3.83	1.15	5393	624	(0.63, 0.35)
PFR2	6.5	2.29	0.80	2792	636	(0.64, 0.33)
PFR3	6.5	1.71	0.57	2193	652	(0.65, 0.32)

[a] At the brightness of 1.0 cd m^{-2} . [b] Maximum values. [c] At the maximum LE. [d] Measured at 8.0 V.

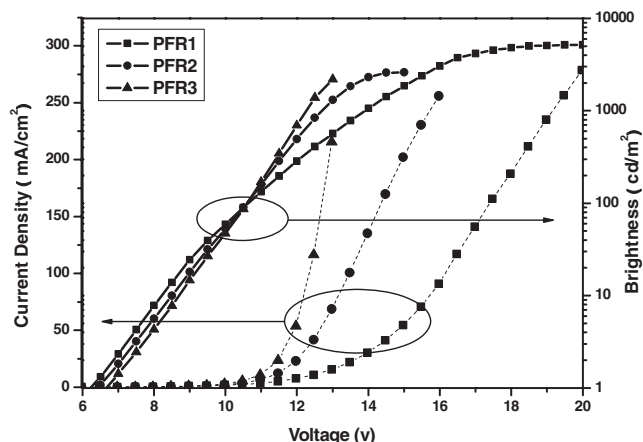


Figure 5. Voltage–current density–brightness curves of the devices of the red polymers.

polymers show high EL efficiencies with pure red emission. For example, the devices of PFR1 shows pure red emission with the CIE coordinates of (0.63, 0.35) at 8.0 V, turn on voltage of 6.5 V, maximum brightness of 5393 cd m^{-2} (Figure 5). At a current density of 3.02 mA cm^{-2} , it exhibits a maximum luminous efficiency of 3.83 cd A^{-1} , power efficiency of 1.09 lm W^{-1} . The devices of PFR2 emits saturated red light with the CIE coordinates of (0.64, 0.33) at 8.0 V, turn on voltage of 6.5 V, maximum brightness of 4453 cd m^{-2} . At a current density of 1.38 mA cm^{-2} , it has a maximum luminous efficiency of 2.29 cd A^{-1} , power efficiency of 0.80 lm W^{-1} . The devices of PFR3 emits deep-red light with the CIE coordinates of (0.65, 0.32) at 8.0 V, turn on voltage of 6.7 V, maximum brightness of 2593 cd m^{-2} . At a current density of 1.74 mA cm^{-2} , it achieves a maximum luminous efficiency of 1.71 cd A^{-1} , power efficiency of 0.57 lm W^{-1} . The devices of PFR1 and PFR2 achieve remarkable EL luminous efficiencies with excellent CIE coordinates, at a brightness of 100 cd m^{-2} , the EL luminous efficiency of PFR1 and PFR2 is up to 3.78 cd A^{-1} and 2.14 cd A^{-1} (Figure 6), which are superior to that of previously reported fluorescent red-light emitting polymer devices. Thus, we have realized highly efficient pure red polymer light-emitting devices with excellent EL efficiency/color purity trade-offs by introduction of these saturated red dopants with fine-tuned PL efficiencies and emission wavelengths.

To further improve the EL performance of the devices of the polymers, we use an alcohol-soluble conjugated polymer, poly[9,9-bis(6'-diethoxyphosphorylhexyl)-fluorene] (PF-EP) as

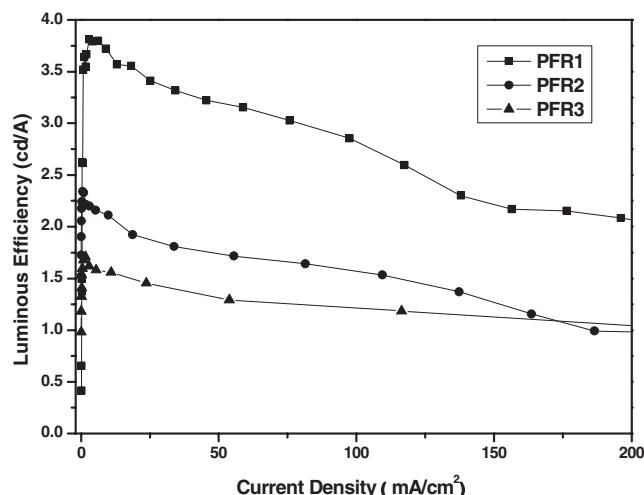


Figure 6. Dependence of the luminous efficiencies on the current densities of the devices of the polymers.

the electron injection layer (EIL) to fabricate two-layer devices of the red polymers with a structure of ITO/PEDOT:PSS(40nm)/EML(80 nm)/PF-EP(10 nm)/LiF(1 nm)/Al(100 nm). The EL performances of the devices of the red polymers using PF-EP as the EIL are summarized in Table 4. The multilayer device of PFR1 shows turn on voltage of 4.5 V, and maximum brightness of 10800 cd cm^{-2} (Figure 7). At a current density of 0.30 mA cm^{-2} , it exhibits a maximum luminous efficiency of 5.50 cd A^{-1} , a maximum power efficiency of 3.14 lm W^{-1} (Figure 8), all of which are superior to the device of PFR1 using Ca/Al as the cathode. The EL efficiencies of the multilayer devices of PFR2 and PFR3 are improved as well. Even at a brightness of 100 cd m^{-2} , the EL luminous efficiency of the multilayer devices of PFR1 and PFR2 still remain as high as 4.45 cd A^{-1} and 2.64 cd A^{-1} . The detailed optimizing mechanism is still in researching, however, the following aspects may contribute to the improvement of the EL performances of the devices: i) Promoted electron injection. PF-EP can facilitate electron injection from the cathode because the phosphonate groups in the pendants have a strong coordinating power to aluminum.^[33,38] ii) Suppressed electrode quenching. It has been proved that the excitons recombination zone is located close to the EML/PF-EP interface,^[39] therefore, the excitons quenching by low band-gap PEDOT and metal cathode can be effectively avoided. Further research about the devices using PE-EP as EIL will be reported later.

Table 4. EL performance of the multilayer devices of the red polymers.

	Turn-on Voltage [V] [a]	Luminous Efficiency [cd A^{-1}] [b]	Power Efficiency [lm W^{-1}] [c]	Maximum Brightness [cd m^{-2}]	EQE [%]	λ_{max} [nm]	CIE (x, y) [d]
PFR1	4.5	5.50	3.14	10800	5.51	624	(0.62, 0.35)
PFR2	4.5	3.10	1.62	6115	3.88	636	(0.63, 0.33)
PFR3	5.0	2.05	0.87	3395	3.37	652	(0.64, 0.32)

[a] At the brightness of 1.0 cd m^{-2} . [b] Maximum values. [c] At the maximum LE. [d] Measured at 6.0 V.

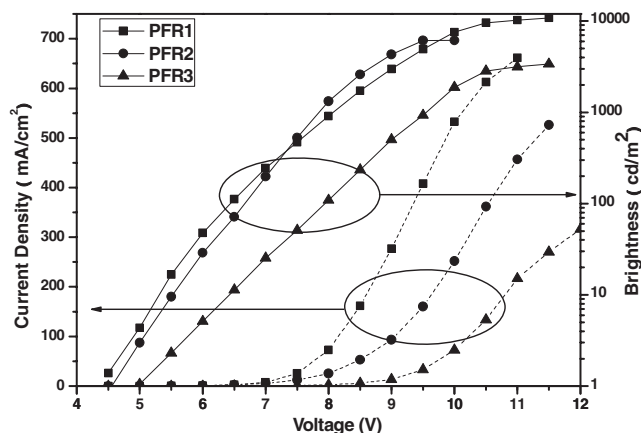


Figure 7. Voltage-current density-brightness curves of the multilayer devices of the red polymers.

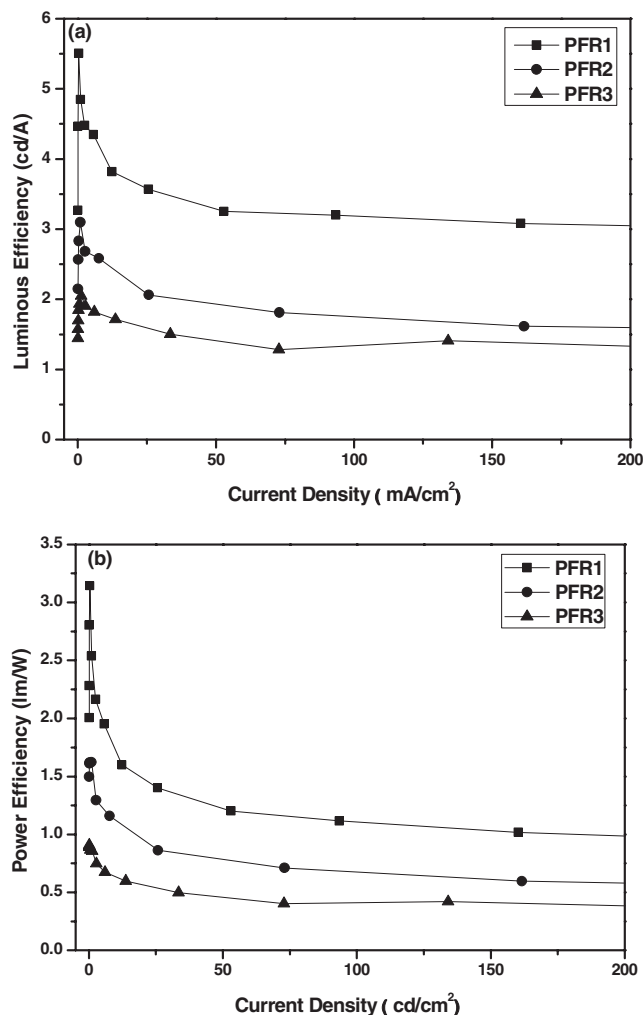


Figure 8. Dependence of the luminous efficiencies (a) and power efficiencies (b) on the current densities of the multilayer devices of the polymers.

3. Conclusions

In conclusion, we have synthesized a series of red EL polymers based on polyfluorene as blue host and 2,1,3-benzothiadiazole derivatives with different emission wavelengths as red dopants on the side chain. By adjusting the electron donating ability of the donor units in these D- π -A-D typed 2,1,3-benzothiadiazole derivatives, the resulting polyfluorene copolymers with fine-tuned PL efficiencies and emission wavelengths led to the optimization of red PLEDs EL efficiency/color purity trade-offs. Pure and saturated red emission single-layer PLED devices (ITO/PEDOT:PSS/Polymer/Ca/Al) are achieved with maximum luminous efficiencies of 3.83 cd A^{-1} and CIE of (0.63, 0.35) for PFR1, 2.29 cd A^{-1} , and CIE of (0.64, 0.33) for PFR2, respectively. By introduction of ethanol soluble PF-EP as the electron injection layer, high performance two-layer devices with the configuration of ITO/PEDOT:PSS/Polymer/PF-EP/LiF/Al show pure red emission at 624 nm with a luminous efficiency of 5.50 cd A^{-1} and CIE of (0.62, 0.35) for PFR1, saturated red emission at 636 nm with a luminous efficiency of 3.10 cd A^{-1} and CIE of (0.63, 0.33) for PFR2, respectively. To the best of our knowledge, these are the best results for pure and saturated red fluorescent polymers reported so far.

4. Experimental Section

Synthesis: All reagents were purchased from Aldrich, Acros, or Alfa and used directly without any further purification. Tetrahydrofuran (THF) used for reaction iv and toluene used for Suzuki polycondensation were purified according to standard procedures. Synthetic routes of 11 and 14 have been reported previously,^[23] 2,7-dibromo-9,9-dioctylfluorene (19) and 2,7-bis-(trimethyleneborate)-9,9-dioctyl-fluorene (20) were prepared according to literature.^[40]

(4-Bromo-phenyl)-di-(4-methoxyphenyl)-amine (1): A mixture of 4-bromobenzenamine (17.2 g, 100 mmol), 1-iodo-4-methoxybenzene (56.2 g, 240 mmol), CuCl (1.0 g, 10 mmol), 1,10-phenanthroline monohydrate (1.9 g, 10 mmol), KOH (28 g, 500 mmol), and *p*-xylene (250 mL) were heated to reflux in a 500 mL bottom flask. After being stirred for 20 h, the reaction mixture was cooled to around 100°C , 2 M HCl was added to the flask slowly, extracted with CH_2Cl_2 and filtered. The organic filtrate was washed with brine and dried with anhydrous Na_2SO_4 . The solvent was removed and the residue was sequentially purified by column chromatography (eluent: petrol ether (PE)/ CH_2Cl_2 5:1) and recrystallization from methanol to afford a white needle crystal. Yield: 15.2 g (56.7%). $^1\text{H NMR}$ (400 MHz, CDCl_3 , δ): 7.23 (br, 2H), 7.02 (br, 4H), 6.82 (d, $J = 8.4 \text{ Hz}$, 6H), 3.79 (s, 6H). MALDI-TOF (m/z): 383.1 [M^+]

(4-(4,4,5,5-Tetramethyl-(1,3,2)dioxaborolan-2-yl)-phenyl)-di-(4-methoxyphenyl)-amine (2): A mixture of 1 (7.7 g, 20 mmol), Pd(dppf) $\text{Cl}_2 \cdot \text{CH}_2\text{Cl}_2$ (0.41 g, 5 mmol), diborane pinacol ester (6.1 g, 24 mmol) and KOAc (6.0 g, 60 mmol) in 100 mL DMF was heated to 80°C for 12 h. After cooling, DMF solvent was removed by vacuum distillation. The reaction mixture was dissolved in CH_2Cl_2 , washed with water and then dried over anhydrous Na_2SO_4 . After removing the solvent, the residue was purified by column chromatography (eluent: PE/ethyl acetate 10:1) to afford a white needle crystal. Yield: 7.1 g (81.2%). $^1\text{H NMR}$ (400 MHz, CDCl_3 , δ): 7.60 (br, 2H), 7.05 (br, 4H), 6.83 (d, $J = 8.0 \text{ Hz}$, 6H), 3.80 (s, 6H), 1.32 (s, 12H). MALDI-TOF (m/z): 431.2 [M^+]

4-(4-(Di-(4-methoxyphenyl)amino)phenyl)-7-bromo-2,1,3-benzothiadiazole (3): A mixture of 2 (3.4 g, 8 mmol), Pd(PPh₃)₄ (0.139 g, 0.12 mmol), 4,7-dibromo-2,1,3-benzothiadiazole (3.6 g, 12 mmol), Aliquat 336 (60 mg) in a two phase solvent of 2 M K_2CO_3 (25 mL) and toluene (75 mL) was heated to 90°C and stirred in dark for 12 h. After cooling, the mixture was washed with brine and dried with anhydrous

Na₂SO₄. The residue was purified by column chromatography (eluent: PE/CH₂Cl₂ 4:1) to give a red solid. Yield: 2.8 g (67.5%). ¹H NMR (400 MHz, CDCl₃, δ): 7.88 (d, *J* = 8.0 Hz, 1H), 7.76 (br, 2H), 7.52 (br, 1H), 7.11 (br, 4H), 6.88 (br, 6H), 3.82 (s, 6H). MALDI-TOF (*m/z*): 517.0 [M⁺]

Tributyl(3,4-ethylenedioxythieryl-2)stannane (4): To a solution of 3,4-ethylenedioxythiophene (7.1 g, 50 mmol) in dry THF (150 mL) at -78 °C, 2.9 M *n*-butyllithium (19.0 mL, 55 mmol, in hexane) was added dropwise. After stirring for 1 h, (*n*-Bu)₃SnCl (16.2 mL, 60 mmol) was added slowly to it. The reaction mixture was warmed up to room temperature and stirred overnight. After removing the THF solvent, the residue was dissolved in PE and filtered. The solvent was evaporated to afford a product of brown oil and the stannic derivative was used without any further purification in the Stille coupling reactions. Yield: 25.4 g (99%). MALDI-TOF (*m/z*): 455.1 [M + ²³Na⁺].

***N*-(4-(*tert*-butyldimethylsilyloxy)phenyl)benzenamine (5):** To a suspension of 4-(phenylamino)phenol (11.1 g, 60 mmol) in CH₂Cl₂ (50 mL) at 0 °C, N(C₂H₅)₃ (10.1 mL, 72 mmol) was added and the suspension became a transparent solution. After stirred for 20 minutes, *tert*-butyldimethylsilylchloride (10.9 g, 72 mmol) dissolved in CH₂Cl₂ (50 mL) was added dropwise. The mixture was warmed to room temperature and stirred overnight. After filtering, the filtrate was washed with water and dried over anhydrous Na₂SO₄. The solvent was evaporated and the residue was purified by column chromatography (eluent: PE/CH₂Cl₂ 3:1) to give a white solid. Yield: 15.4 g (86.4%). ¹H NMR (300 MHz, DMSO-*d*₆, δ): 7.85 (s, 1H), 7.16 (t, *J* = 8.0 Hz, 2H), 7.00–6.92 (m, 4H), 6.77–6.69 (m, 3H), 0.95 (s, 9H), 0.17 (s, 6H). MALDI-TOF (*m/z*): 299.2 [M⁺]

4-Bromo-*N*-(4-(*tert*-butyldimethylsilyloxy)-phenyl)-*N*-phenylbenzenamine (6): 6 was synthesized according to literature.^[41] A solution of 5 (6.0 g, 20 mmol), 1-bromo-4-iodobenzene (14.2 g, 50 mmol), Pd₂(dba)₃ (0.061 g, 0.067 mmol), *rac*-binap (0.124 g, 0.200 mmol), NaOBu-*t* (3.8 g, 40 mmol) in toluene (100 mL) was stirred vigorously overnight at 100 °C. The reaction mixture was then cooled to room temperature and filtered. The filtrate was washed with water, dried over anhydrous Na₂SO₄, concentrated in vacuo to give a colorless solid. The residue was then purified by column chromatography (eluent: PE/CH₂Cl₂ 6:1) to afford a colorless oil. Yield: 1.3 g (57.6%). ¹H NMR (400 MHz, CDCl₃, δ): 7.64 (d, *J* = 8.0 Hz, 2H), 7.23 (t, *J* = 8.0 Hz, 2H), 7.07 (d, *J* = 8.0 Hz, 2H), 7.01–6.95 (m, 5H), 6.76 (d, *J* = 8.4 Hz, 2H), 0.99 (s, 9H), 0.21 (s, 6H).

2-(4-(*N*-Phenyl-*N*-(4-(*tert*-butyldimethylsilyloxy)phenylamino)phenylthiophene (7): A mixture of 6 (1.2 g, 2.4 mmol), tributyl(thiophen-2-yl)stannane (0.74 g, 2.0 mmol), Pd(PPh₃)₄ (22.5 mg, 0.01 mmol) and toluene (30 mL) was heated to 100 °C and stirred in the dark for 24 h. After workup, the mixture was poured to saturated aqueous KF and stirred vigorously for 3 h to remove the residual noxious organic stannic derivatives. After filtering, the filtrate was extracted with diethyl ether, washed with brine and dried with anhydrous Na₂SO₄. The residue was purified by column chromatography (eluent: PE/CH₂Cl₂ 5:1) to afford an olive oil. Yield: 0.74 g (82.1%). ¹H NMR (400 MHz, CDCl₃, δ): 7.44 (d, *J* = 8.8 Hz, 2H), 7.23–7.19 (m, 4H), 7.08–6.96 (d, 8H), 6.77 (d, *J* = 8.8 Hz, 2H), 0.99 (s, 9H), 0.21 (s, 6H). MALDI-TOF (*m/z*): 457.2 [M⁺]

Tributyl(5-(4-(*N*-phenyl-*N*-(4-(*tert*-butyldimethylsilyloxy)phenylamino)phenyl)-thienyl-2)stannane (8): Compound 8 was synthesized following the same procedure for 4 using 7 instead of 3,4-ethylenedioxythiophene to give a brown oil. Yield: 1.2 g (99%). MALDI-TOF (*m/z*): 747.3 [M⁺]

2-(4-(*N*-Phenyl-*N*-(4-(*tert*-butyldimethylsilyloxy)phenylamino)phenyl)-3,4-ethylenedioxythiophene (9): Compound 9 was synthesized following the same procedure for 7 using 4 instead of tributyl(thienyl-2)stannane to give a yellow solid. Yield: 4.6 g (78.6%). ¹H NMR (300 MHz, CDCl₃, δ): 7.54 (d, *J* = 8.7 Hz, 2H), 7.21 (t, *J* = 8.2 Hz, 2H), 7.07–6.93 (m, 7H), 7.76 (d, *J* = 8.7 Hz, 2H), 6.23 (s, 1H), 4.29–4.20 (m, 4H), 0.99 (s, 9H), 0.21 (s, 6H). MALDI-TOF (*m/z*): 515.3 [M⁺]

Tributyl(5-(4-(*N*-phenyl-*N*-(4-(*tert*-butyldimethylsilyloxy)phenylamino)phenyl)-3,4-ethylenedioxythienyl-2)stannane (10): Compound 10 was synthesized following the same procedure for 4 using 9 instead of 3,4-ethylenedioxythiophene to give a brown oil. Yield: 4.5 g (99%). MALDI-TOF (*m/z*): 805.1 [M⁺]

4-(5-(4-(*N*-Phenyl-*N*-(4-(*tert*-butyldimethylsilyloxy)phenylamino)phenyl)-3,4-ethylenedioxythienyl-2)-7-(4-(diphenylamino)phenyl)-2,1,

3-benzothiadiazole (12): Compound 12 was synthesized following the same procedure for 7 using 11 and 10 instead of 6 and tributyl(thiophen-2-yl)stannane to give a violet-red solid. Yield: 1.5 g (95.1%). ¹H NMR (300 MHz, CDCl₃, δ): 8.44 (d, *J* = 7.5 Hz, 1H), 7.89 (d, *J* = 8.7 Hz, 2H), 7.71 (dd, *J* = 5.6 Hz, 2H), 7.32–7.18 (m, 13H), 7.10–6.96 (m, 9H), 6.78 (d, *J* = 8.7 Hz, 2H), 4.47–4.40 (m, 4H), 1.00 (s, 9H), 0.22 (s, 6H). MALDI-TOF (*m/z*): 892.3 [M⁺]

4-(5-(4-(*N*-Phenyl-*N*-(4-(hydroxyphenyl)amino)phenyl)-3,4-ethylenedioxythienyl-2)-7-(4-(diphenylamino)phenyl)-2,1,3-benzothiadiazole (13): A mixture of 12 (0.72 g, 0.83 mmol), 6 M HCl (30 mL) and THF (60 mL) was stirred vigorously overnight. After workup, the reaction mixture was extracted with CH₂Cl₂, washed with brine and dried over anhydrous Na₂SO₄. The residue was purified by column chromatography (eluent: CH₂Cl₂) to afford a violet-red solid. Yield: 0.7 g (94.7%). ¹H NMR (400 MHz, CDCl₃, δ): 7.88 (br, 3H), 7.70 (br, 3H), 7.29 (d, *J* = 8.0 Hz, 6H), 7.22–7.18 (m, 10H), 7.05 (br, 4H), 7.11–7.04 (m, 4H), 6.78 (br, 3H), 4.46 (br, 4H). MALDI-TOF (*m/z*): 778.2 [M⁺]

4-(5-(4-(*N*-Phenyl-*N*-(4-(*tert*-butyldimethylsilyloxy)phenylamino)phenyl)-thienyl-2)-7-(4-(di-(4-methoxyphenyl)-amino)phenyl)-2,1,3-benzothiadiazole (15): Compound 15 was synthesized following the same procedure for 7 using 3 and 8 instead of 6 and tributyl(thiophen-2-yl)stannane to give a deep-red solid. Yield: 0.87 g (95.7%). ¹H NMR (300 MHz, CDCl₃, δ): 8.09 (s, 1H), 7.90 (d, *J* = 7.2 Hz, 1H), 7.82 (d, *J* = 8.4 Hz, 2H), 7.66 (d, *J* = 6.6 Hz, 2H), 7.54 (d, *J* = 8.4 Hz, 2H), 7.33–7.23 (m, 4H), 7.11–7.02 (m, 4H), 6.87 (d, *J* = 9.3 Hz, 2H), 6.79 (d, *J* = 8.7 Hz, 2H), 3.82 (s, 6H), 1.00 (s, 9H), 0.22 (s, 6H). MALDI-TOF (*m/z*): 894.3 [M⁺]

4-(5-(4-(*N*-Phenyl-*N*-(4-(hydroxyphenyl)amino)phenyl)-thienyl-2)-7-(4-(di-(4-methoxyphenyl)-amino)-phenyl)-2,1,3-benzothiadiazole (16): Compound 16 was synthesized following the same procedure for 13 using 15 instead of 12 to give a deep-red solid. Yield: 0.65 g (92.3%). ¹H NMR (400 MHz, CDCl₃, δ): 8.10 (br, 2H), 7.82 (d, *J* = 8.0 Hz, 4H), 7.67 (br, 3H), 7.13 (br, 6H), 7.05 (br, 4H), 6.87 (d, *J* = 8.4 Hz, 7H), 6.78 (br, 3H), 3.82 (s, 6H). MALDI-TOF (*m/z*): 780.2 [M⁺]

4-(5-(4-(*N*-Phenyl-*N*-(4-(*tert*-butyldimethylsilyloxy)phenylamino)phenyl)-3,4-ethylenedioxythienyl-2)-7-(4-(di-(4-methoxyphenyl)-amino)phenyl)-2,1,3-benzothiadiazole (17): Compound 17 was synthesized following the same procedure for 7 using 3 and 10 instead of 6 and tributyl(thiophen-2-yl)stannane to give a violet-red solid. Yield: 2.0 g (94.2%). ¹H NMR (400 MHz, CDCl₃, δ): 7.82 (d, *J* = 8.4 Hz, 2H), 7.68 (d, *J* = 7.6 Hz, 3H), 7.23 (d, *J* = 7.6 Hz, 2H), 7.13 (d, *J* = 8.8 Hz, 5H), 7.09–6.99 (m, *J* = 8.8 Hz, 9H), 6.86 (d, *J* = 9.2 Hz, 5H), 6.77 (d, *J* = 8.4 Hz, 2H), 4.46 (br, 4H), 3.82 (s, 6H), 1.00 (s, 9H), 0.22 (s, 6H). MALDI-TOF (*m/z*): 952.3 [M⁺]

4-(5-(4-(*N*-Phenyl-*N*-(4-(hydroxyphenyl)amino)phenyl)-3,4-ethylenedioxythienyl-2)-7-(4-(di-(4-methoxyphenyl)amino)phenyl)-2,1,3-benzothiadiazole (18): Compound 18 was synthesized following the same procedure for 13 using 17 instead of 12 to give a violet-red solid. Yield: 1.1 g (92.5%). ¹H NMR (400 MHz, CDCl₃, δ): 7.81 (br, 3H), 7.71 (br, 4H), 7.13 (d, *J* = 8.8 Hz, 6H), 7.05 (d, *J* = 8.4 Hz, 4H), 6.86 (d, *J* = 8.8 Hz, 7H), 6.78 (br, H), 4.46 (br, 4H), 3.82 (s, 6H). MALDI-TOF (*m/z*): 838.2 [M⁺]

4-(5-(4-(*N*-Phenyl-*N*-(4-methoxyphenyl)amino)phenyl)-thienyl-2)-7-(4-(di-(4-methoxyphenyl)amino)phenyl)-2,1,3-benzothiadiazole (MCR1): A mixture of 16 (0.16 g, 0.20 mmol), K₂CO₃ (1.38 g, 10.00 mmol), CH₃I (2.00 mL, 32.10 mmol) and acetone (50 mL) was heated to 60 °C for 6 h. After workup, the acetone solvent was evaporated, the mixture was extracted with CH₂Cl₂ and filtered. The filtrate was evaporated and the residue was purified by flash column chromatography (eluent: CH₂Cl₂) to afford a deep-red solid. Yield: 0.15 g (95.7%). ¹H NMR (400 MHz, CDCl₃, δ): 8.10 (d, *J* = 3.6 Hz, 1H), 7.89 (d, *J* = 7.6 Hz, 1H), 7.83 (d, *J* = 8.8 Hz, 2H), 7.66 (d, *J* = 7.6 Hz, 1H), 7.54 (d, *J* = 8.8 Hz, 2H), 7.31 (d, *J* = 4.0 Hz, 1H), 7.26 (t, *J* = 8.0 Hz, 2H), 7.16–7.10 (m, 8H), 7.07–6.97 (m, 5H), 6.87 (dd, *J* = 5.8 Hz, 6H), 3.82 (s, 9H). Anal. Calcd. For C₄₉H₃₈N₄O₄S₂: C, 74.03; H, 4.82; N, 7.05; Found: C, 73.85; H, 4.94; N, 6.98. MALDI-TOF (*m/z*): 794.2 [M⁺]

4-(5-(4-(*N*-Phenyl-*N*-(4-methoxyphenyl)amino)phenyl)-3,4-ethylenedioxythienyl-2)-7-(4-(diphenylamino)phenyl)-2,1,3-benzothiadiazole

(MCR2): MCR2 was synthesized following the same procedure for MCR1 using 13 instead of 16 to give a violet-red solid. Yield: 0.37 g (98.2%). $^1\text{H NMR}$ (400 MHz, CDCl_3 , δ): 8.44 (d, $J = 8.0$ Hz, 1H), 7.89 (d, $J = 4.8$ Hz, 2H), 7.71 (dd, $J = 5.6$ Hz, 2H), 7.31–7.18 (m, 13H), 7.12–7.04 (m, 8H), 6.98 (t, $J = 7.2$ Hz, 1H), 6.86 (d, $J = 5.2$ Hz, 2H), 4.47–4.39 (m, 4H), 3.82 (s, 9H). Anal. Calcd. For $\text{C}_{49}\text{H}_{36}\text{N}_4\text{O}_3\text{S}_2$: C, 74.22; H, 4.58; N, 7.07; Found: C, 73.95; H, 4.62; N, 6.98. MALDI-TOF (m/z): 792.2 [M^+]

4-(5-(4-(*N*-Phenyl-*N*-(4-methoxyphenyl)amino)phenyl)-3,4-ethylenedioxythienyl)-7-(4-(di-(4-methoxyphenyl)-amino)phenyl)-2,1,3-benzothiadiazole (MCR3): MCR3 was synthesized following the same procedure for MCR1 using 18 instead of 16 to give a violet-red solid. Yield: 0.36 g (98.5%). $^1\text{H NMR}$ (400 MHz, CDCl_3 , δ): 8.42 (d, $J = 8.0$ Hz, 1H), 7.83 (d, $J = 8.8$ Hz, 2H), 7.69 (t, $J = 8.4$ Hz, 3H), 7.24 (t, $J = 8.6$ Hz, 2H), 7.15–7.04 (m, 12H), 6.98 (t, $J = 7.2$ Hz, 1H), 6.86 (d, $J = 8.8$ Hz, 6H), 4.46–4.40 (m, 4H), 3.82 (s, 9H). Anal. Calcd. For $\text{C}_{51}\text{H}_{40}\text{N}_4\text{O}_5\text{S}_2$: C, 71.81; H, 4.73; N, 6.57; Found: C, 71.39; H, 4.81; N, 6.51. MALDI-TOF (m/z): 852.2 [M^+]

Monomer R1: Monomer R1 was synthesized using the same reaction conditions as Suzuki coupling for 3. Here it is a reaction between a brominated alkane and a phenolic hydroxyl group to give a alkyl aryl ether, and can be effectively catalyzed by $\text{Pd}(\text{PPh}_3)_4$. The residue was purified by column chromatography (eluent: $\text{PE}/\text{CH}_2\text{Cl}_2$ 1:1) to afford a deep-red solid. Yield: 0.65 g (85.6%). $^1\text{H NMR}$ (300 MHz, CDCl_3 , δ): 8.09 (br, 1H), 7.84 (br, 3H), 7.66 (br, 1H), 7.53 (d, $J = 8.4$ Hz, 4H), 7.46 (d, $J = 5.7$ Hz, 4H), 7.32–7.08 (m, 15H), 6.89–6.79 (m, 7H), 3.82 (s, 8H), 1.97–1.89 (m, 4H), 1.65–1.56 (m, 2H), 1.26–1.05 (m, 10H), 0.88–0.76 (m, 5H) 0.61 (br, 4H). Anal. Calcd. For $\text{C}_{73}\text{H}_{66}\text{Br}_2\text{N}_4\text{O}_3\text{S}_2$: C, 68.97; H, 5.23; N, 4.41; Found: C, 69.43; H, 5.25; N, 4.37. MALDI-TOF (m/z): 1268.3 [M^+]

Monomer R2: Monomer R2 was synthesized following the same procedure for Monomer R1 using 13 instead of 16 to give a violet-red solid. Yield: 0.45 g (81.2%). $^1\text{H NMR}$ (300 MHz, CDCl_3 , δ): 7.89 (br, 2H), 7.70 (br, 3H), 7.52 (d, $J = 8.7$ Hz, 2H), 7.47–7.44 (m, 4H), 7.29–7.27 (m, 6H), 7.20 (t, $J = 7.2$ Hz, 9H), 7.06 (t, $J = 7.2$ Hz, 4H), 6.80 (br, 5H), 4.47 (br, 4H), 3.82 (s, 2H), 1.97–1.89 (m, 4H), 1.65–1.56 (m, 2H), 1.26–1.05 (m, 10H), 0.88–0.76 (m, 5H), 0.61 (br, 4H). Anal. Calcd. For $\text{C}_{73}\text{H}_{64}\text{Br}_2\text{N}_4\text{O}_3\text{S}_2$: C, 69.08; H, 5.08; N, 4.41; Found: C, 69.13; H, 5.14; N, 4.38. MALDI-TOF (m/z): 1266.3 [M^+]

Monomer R3: Monomer R3 was synthesized following the same procedure for Monomer R1 using 18 instead of 16 to give a violet-red solid. Yield: 0.77 g (83.5%). $^1\text{H NMR}$ (300 MHz, CDCl_3 , δ): 7.82 (br, 2H), 7.70 (br, 3H), 7.52 (d, $J = 8.7$ Hz, 2H), 7.47–7.44 (m, 4H), 7.33 (t, $J = 2.4$ Hz, 1H), 7.13 (br, 12H), 6.86 (d, $J = 8.1$ Hz, 4H), 6.80 (br, 3H), 4.47 (br, 4H), 3.82 (s, 8H), 1.97–1.89 (m, 4H), 1.65–1.56 (m, 2H), 1.26–1.05 (m, 10H), 0.88–0.76 (m, 5H) 0.61 (br, 4H). Anal. Calcd. $\text{C}_{75}\text{H}_{68}\text{Br}_2\text{N}_4\text{O}_5\text{S}_2$: C, 67.76; H, 5.16; N, 4.21; Found: C, 68.13; H, 5.24; N, 4.16. MALDI-TOF (m/z): 1326.3 [M^+]

General Procedure of the Suzuki Polycondensation: A mixture of 2,7-dibromo-9,9-dioctylfluorene (18), 2,7-bis-(1,3,2-dioxaborinane-2-yl)-9,9-dioctylfluorene (19) and corresponding red-unit-containing comonomer with corresponding feed ratios, Aliquat 336 (0.10 g, 0.25 mmol), $\text{Pd}(\text{PPh}_3)_4$ (11.0 mg, 0.01 mmol) under argon was added degassed 2 M aqueous K_2CO_3 (2 mL) and degassed toluene (6 mL). The resulting mixture was stirred in the dark at 90 °C for 48 h, and then sequentially end-capped with 0.1 M phenylboronic acid (2 mL) and bromobenzene (1 mL), stirring for 12 h for each addition. After cooling, the reaction mixture was poured into methanol and filtered. The precipitate was collected and dissolved in CH_2Cl_2 , washed with water and dried with anhydrous Na_2SO_4 . After evaporating most of the solvent, the residue was precipitated in stirred methanol solvent to give a fiber-like solid. The polymer was further purified by Soxhlet extraction with acetone for 24 h. The reprecipitation procedure in CH_2Cl_2 -methanol was then repeated several times. The final product was obtained after drying in vacuum with a yield of 56%–70%.

PFO: light yellow fiber. 19 (0.2742 g, 0.500 mmol) and 20 (0.2742 g, 0.500 mmol) were used in the polymerization. GPC: $M_n = 4.1 \times 10^4$, PDI = 2.5. $^1\text{H NMR}$ (300 MHz, CDCl_3 , δ): 7.85 (d, 2H), 7.72 (br, 4H), 2.12 (br, 4H), 1.14 (br, 24H), 0.82 (t, 6H). Anal. Calcd: C, 89.69; H, 10.31. Found: C, 89.08; H, 10.02. PFR1: red fiber. 19 (0.2726 g, 0.497 mmol),

20 (0.2792 g, 0.500 mmol) and Monomer R1 (0.0038 g, 0.003 mmol) were used in the polymerization. GPC: $M_n = 4.7 \times 10^4$, PDI = 2.5. PFR2: red fiber. 19 (0.2726 g, 0.497 mmol), 20 (0.2792 g, 0.500 mmol) and Monomer R2 (0.0038 g, 0.003 mmol) were used in the polymerization. GPC: $M_n = 3.7 \times 10^4$, PDI = 2.9. PFR3: violet-red fiber. 19 (0.2726 g, 0.497 mmol), 20 (0.2792 g, 0.500 mmol) and Monomer R3 (0.0040 g, 0.003 mmol) were used in the polymerization. GPC: $M_n = 5.3 \times 10^4$, PDI = 2.5. PFR1, PFR2 and PFR3 showed similar $^1\text{H NMR}$ and element analysis results as those of PFO.

Measurement and Characterization: $^1\text{H NMR}$ spectra were recorded with a Bruker AV300 or AV400 NMR spectrometer. The elemental analyses were performed using a Bio-Rad elemental analysis system. The number- and weight-average molecular weights of the polymers were determined by gel permeation chromatography (GPC) using a Waters 410 instrument with polystyrene as standard and THF as eluent. UV-Vis absorption spectra were measured by a Perkin-Elmer Lambda 35 UV/Vis spectrometer. PL spectra were recorded by a Perkin-Elmer LS50B spectrofluorometer. MALDI-TOF was measured by a Bruker Daltonics Flexanalysis system. Cyclic voltammograms of polymer films on glassy carbon electrodes were recorded on an EG&G 283 (Princeton Applied Research) potentiostat/galvanostat system at room temperature in a solution of *n*-Bu₄NClO₄ (0.10 M) in fresh acetonitrile at a scan rate of 100 mV/s. A Pt wire and an Ag/AgCl electrode were used as the counter electrode and the reference electrode, respectively. Cyclic voltammograms of small organic molecules were carried out with their solution in fresh CH_2Cl_2 . Other conditions were the same as for polymer films except that a Pt disc was used as the working electrode. The EL spectra and current–voltage and brightness–voltage characteristics of the devices were measured with a Spectrascan PR650 spectrophotometer in the forward direction and a computer-controlled Keithley 2400 instrument under ambient conditions. The external quantum yields were calculated from the brightness, current density and EL spectrum, assuming a Lambertian distribution.

Device Fabrication: ITO glass plates were degreased in an ultrasonic acetone solvent bath and then dried in a heating chamber at 120 °C. The PEDOT:PSS was spin-coated on the cleaned ITO at 3000 rpm for 60 s and then baked for 20 min at 120 °C to give an approximate thickness of 40 nm. The polymer layer (approximately 90 nm) was then spin-coated on to the PEDOT/ITO coated glass substrate in fresh toluene solution (15 mg mL⁻¹) under ambient atmosphere. Finally, a thin layer of calcium (10 nm) followed by a layer of aluminium (100 nm) was deposited in a vacuum thermal evaporator or through a shadow mask at a pressure of 3×10^{-3} – 5×10^{-3} Pa. The active area of the diodes was around 12 mm². For the multilayer device, PF-EP was spin coated on the emissive layer from ethanol (3 mg/mL⁻¹) and annealed at 70 °C for 30 min. Then 1 nm of LiF and 100 nm of Al were deposited at a pressure of 4×10^{-4} Pa successively.

Acknowledgements

This work was supported by the Changchun Institute of Applied Chemistry, Chinese Academy of Sciences (CX07QZJC-24), the National Natural Science Foundation of China (No.50803062, 60977026), the Science Fund for Creative Research Groups (No.20621401), and the 973 Project (2009CB623601).

Received: April 28, 2010
Published online: July 29, 2010

- [1] H. Burroughes, D. D. C. Bradley, A. R. Brown, R. N. Marks, K. Mackay, R. H. Friend, P. L. Burns, A. B. Holmes, *Nature* **1990**, 347, 539.
- [2] A. C. Grimsdale, K. Müllen, *Adv. Polym. Sci.* **2006**, 199, 1.
- [3] A. Kraft, A. C. Grimsdale, A. B. Holmes, *Angew. Chem. Int. Ed.* **1998**, 37, 402.

- [4] M. T. Bernius, M. Inbasekaran, J. O. Brien, W. S. Wu, *Adv. Mater.* **2000**, *12*, 1767.
- [5] K. T. Kamtekar, A. P. Monkman, M. R. Bryce, *Adv. Mater.* **2010**, *22*, 572.
- [6] W. S. Wu, M. Inbasekaran, M. Hudack, D. Welsh, W. L. Yu, Y. Cheng, C. Wang, S. Kram, M. Tacey, M. Bernius, R. Fletcher, K. Kiszka, S. Munger, J. O. Brien, *Microelectron. J.* **2004**, *35*, 343.
- [7] Q. Hou, Y. S. Xu, W. Yang, M. Yuan, J. B. Peng, Y. Cao, *J. Mater. Chem.* **2006**, *16*, 1431.
- [8] Q. Hou, Q. M. Zhou, Y. Zhang, W. Yang, R. Q. Yang, Y. Cao, *Macromolecules* **2004**, *37*, 6299.
- [9] R. Q. Yang, R. Y. Tian, J. A. Yan, Y. Zhang, J. Yang, Q. Hou, W. Yang, C. Zhang, Y. Cao, *Macromolecules* **2005**, *38*, 244.
- [10] R. Q. Yang, R. Y. Tian, Q. Hou, W. Yang, Y. Cao, *Macromolecules* **2003**, *36*, 7453.
- [11] J. Luo, Q. Hou, J. W. Chen, Y. Cao, *Synth. Met.* **2006**, *156*, 470.
- [12] J. Yang, C. Y. Jiang, Y. Zhang, R. Q. Yang, W. Yang, Q. Hou, Y. Cao, *Macromolecules* **2004**, *37*, 1211.
- [13] N. S. Cho, D. H. Hwang, B. J. Jung, E. Lim, J. Lee, H. K. Shim, *Macromolecules* **2004**, *37*, 5265.
- [14] N. S. Cho, D. H. Hwang, J. I. Lee, B. J. Jung, H. K. Shim, *Macromolecules* **2002**, *35*, 1224.
- [15] L. H. Chan, Y. D. Lee, C. T. Chen, *Macromolecules* **2006**, *39*, 3262.
- [16] N. S. Cho, J. H. Park, S. K. Lee, J. Lee, H. K. Shim, M. J. Park, D. H. Hwang, B. J. Jung, *Macromolecules* **2006**, *39*, 177.
- [17] C. Ego, D. Marsitzky, S. Becker, J. Y. Zhang, A. C. Grimsdale, K. Müllen, J. D. MacKenzie, C. Silva, R. H. Friend, *J. Am. Chem. Soc.* **2003**, *125*, 437.
- [18] C. T. Chen, *Chem. Mater.* **2004**, *16*, 4389.
- [19] E. G. Wang, C. Li, W. L. Zhuang, J. B. Peng, Y. Cao, *J. Mater. Chem.* **2008**, *18*, 797.
- [20] M. J. Park, J. Lee, I. H. Jung, J. H. Park, D. H. Hwang, H. K. Shim, *Macromolecules* **2008**, *41*, 9643.
- [21] J. Liu, J. X. Cao, S. Y. Shao, Z. Y. Xie, Y. X. Cheng, Y. H. Geng, L. X. Wang, X. B. Jing, F. S. Wang, *J. Mater. Chem.* **2008**, *18*, 1659.
- [22] J. Liu, L. J. Bu, J. P. Dong, Q. G. Zhou, Y. H. Geng, D. G. Ma, L. X. Wang, X. B. Jing, F. S. Wang, *J. Mater. Chem.* **2006**, *16*, 1431.
- [23] J. Liu, L. Chen, S. Y. Shao, Z. Y. Xie, Y. X. Cheng, Y. H. Geng, L. X. Wang, X. B. Jing, F. S. Wang, *J. Mater. Chem.* **2008**, *18*, 319.
- [24] J. Liu, S. Y. Shao, L. Chen, Z. Y. Xie, Y. X. Cheng, Y. X. Geng, L. X. Wang, X. B. Jing, F. S. Wang, *Adv. Mater.* **2007**, *19*, 1859.
- [25] J. Liu, Z. Y. Xie, Y. X. Cheng, Y. X. Geng, L. X. Wang, X. B. Jing, F. S. Wang, *Adv. Mater.* **2007**, *19*, 531.
- [26] J. R. Gong, L. J. Wan, S. B. Lei, C. L. Bai, *J. Phys. Chem. B* **2005**, *109*, 1675.
- [27] G. Y. Zhong, Z. Xu, J. He, S. T. Zhang, Y. Q. Zhan, X. J. Wang, Z. H. Xiong, H. Z. Shi, X. M. Ding, *Appl. Phys. Lett.* **2002**, *81*, 1122.
- [28] S. C. Chang, G. He, F. C. Chen, T. F. Tuo, Y. Yang, *Appl. Phys. Lett.* **2001**, *79*, 2088.
- [29] C. C. Huang, H. F. Meng, G. K. Ho, C. H. Chen, *Appl. Phys. Lett.* **2004**, *84*, 1195.
- [30] M. Granström, O. Inganäs, *Appl. Phys. Lett.* **1996**, *68*, 147.
- [31] C. J. Liang, W. C. H. Choy, *J. Organomet. Chem.* **2009**, *694*, 2712.
- [32] J. Kalinowski, P. Di Marco, M. Cocchi, V. Fattori, N. Camaioni, *Appl. Phys. Lett.* **1996**, *68*, 2317.
- [33] G. Zhou, Y. H. Geng, Y. X. Cheng, Z. Y. Xie, L. X. Wang, X. B. Jing, F. S. Wang, *Appl. Phys. Lett.* **2006**, *89*, 233501.
- [34] J. Liu, Z. Y. Xie, Y. X. Cheng, Y. X. Geng, L. X. Wang, X. B. Jing, F. S. Wang, *Adv. Mater.* **2008**, *20*, 1357.
- [35] J. M. Raimundo, P. Blanchard, H. Brisset, S. Akoudad, J. Roncali, *Chem. Commun.* **2000**, 939.
- [36] T. C. Tsai, W. Y. Hung, L. C. Chi, K. T. Wong, C. C. Hsieh, P. T. Chou, *Org. Electron.* **2009**, *19*, 158.
- [37] K. R. Radke, K. Ogawa, S. C. Rasmussen, *Org. Lett.* **2005**, *7*, 5253.
- [38] X. Guo, B. Yao, G. X. Jiang, Y. X. Cheng, Z. Y. Xie, L. X. Wang, X. B. Jing, F. S. Wang, *J. Polym. Sci., Part A: Polym. Chem.* **2008**, *46*, 4866.
- [39] X. D. Niu, C. J. Qin, B. H. Zhang, J. W. Yang, Z. Y. Xie, L. X. Wang, X. B. Jing, F. S. Wang, *Appl. Phys. Lett.* **2007**, *90*, 203513.
- [40] X. W. Chen, J. L. Liao, Y. M. Liang, M. O. Ahmed, H. E. Tseng, S. A. Chen, *J. Am. Chem. Soc.* **2003**, *125*, 636.
- [41] R. Anémian, D. C. Cupertino, P. R. Mackie, S. G. Yeates, *Tetrahedron Lett.* **2005**, *46*, 6717.